Extrusion of Paste Through Non-Axisymmetric Systems

P. J. Martin, D. I. Wilson and K. Challis*

Department of Chemical Engineering
University of Cambridge
Cambridge CB2 3RA, United Kingdom

* Syngenta
Earls Rd, Grangemouth FK3 8XG, United Kingdom

An effective understanding of paste extrusion through axisymmetric barrel and die geometries has been achieved by models such as that described by Benbow and Bridgwater [1]. Experimental and modeling work has been conducted on simple non-axisymmtric systems. An experimental ram extrusion apparatus has been constructed with three nominally identical dies situated at the end of a barrel. Each die can be blocked or left open and five different combinations of flow patterns – axial, axial/radial and radial – have been investigated.

Flow of a talc-based model industrial agrochemical paste has been studied. The rheological behaviour of the paste has been characterized using the Benbow-Bridgwater approach. Paste was forced through each of the barrel and die arrangements using a piston over a range of velocities. Extrudate flow rates, paste flow patterns and stress states were recorded in each case. Dramatic changes in flow pattern have been observed as the paste flow rate was varied for some arrangements.

The extrusion systems have been modeled using a modified Benbow-Bridgwater model. This model has been found to successfully predict the experimental extrusion pressures, but not the observed flow patterns.

INTRODUCTION

Benbow and Bridgwater [1] describe a simple model for the flow of pastes in a ram extruder (Figure 1). If the material is thought to behave as a perfect plastic in the bulk, and the work done in the die entry region is identical to that for homogeneous compression, the die entry pressure drop is given by

$$P_1 = 2\sigma_y \ln(D_0/D) \quad (1)$$

where σ_y is the uniaxial yield stress, D_0 is the barrel diameter, and D is the die land diameter; it is assumed that the barrel and die land both have circular cross-sections. Ovenston and Benbow [2] and Benbow [3] present experimental results for the extrusion of ceramic pastes through square and conical entry dies, and argue that the effect of geometry on the die entry pressure drop is consistent with equation (1).

In homogeneous compression, a rectangular element in the undeformed specimen, with sides parallel to the principal directions of stress and strain, remains rectangular in the deformed state. In this case, all the energy supplied via the platens results in a change in the height of the specimen, and the work done is a minimum. During extrusion, the deformation in the die entry region is not homogeneous, with additional work going into shearing material elements without causing a reduction in the overall diameter. Thus the actual die entry pressure drop is greater than that predicted by equation (1).

It is often found experimentally that P_1 exhibits some rate dependence, and equation (1) is modified by Benbow and Bridgwater [1] as follows:

$$P_1 = 2\left(\sigma_0 + \alpha V^m\right)\ln(D_0/D) \quad (2)$$

where V is the velocity of the paste in the die land, σ_0 is an initial yield stress, and α and m are parameters characterizing the effect of velocity on the die entry. All of σ_0, α and m are regarded as material constants characterizing the material's resistance to change in cross-sectional area in the die entry, and are assumed to be independent of die geometry and extrusion rate.

In the die land the paste flows as a rigid plug, possibly surrounded by a thin layer of lubricating liquid separating it from the wall. Thus, the wall shear stress may be a function of the velocity of the plug, and the die land pressure drop is given by

$$P_2 = 4\left(\tau_0 + \beta V^n\right)L/D \quad (3)$$

where L is the die land length, τ_0 is an initial wall stress, and β and n are parameters characterizing the effect of velocity in the die land; τ_0, β and n are also regarded as material constants. Adding the pressure drops (2) and (3) together leads to the six-parameter model for the overall pressure drop, sometimes known as the Benbow-Bridgwater equation.

$$P = 2\left(\sigma_0 + aV^m\right)\ln\left(D_0/D\right) + 4\left(\tau_0 + \beta V^n\right)L/D \tag{4}$$

The Benbow-Bridgwater model has provided a good first order model for axisymmetric extrusion and provides reasonable industrial design information, although the assumptions involved in the analysis make its precision low. The model is sometimes used to ascertain material constants for more general use. In this case the material constant σ_0 is often thought to be equal to the uniaxial yield stress of the material. Horrobin and Nedderman [4] performed finite element analysis of axially symmetric extrusion of perfect plastics. Writing ξ for $\ln(D_0/D)$ they found that the die entry pressure drop for the case of perfectly smooth walls can be well approximated by the best-fit parabola and straight line

$$P_1 = 0.700\left(\sqrt{26.8\xi + 1} - 1\right)\sigma_y$$

$$D_0/D < 2.5,\ \xi < 0.92 \tag{5}$$

$$P_1 = \left(1.92\xi + 1.08\right)\sigma_y$$

$$D_0/D \geq 2.5,\ \xi \geq 0.92. \tag{6}$$

The straight line for large reductions has a slope that is slightly less than two, and thus approaches the ideal work line as the reduction increases. Hence for large diameter reductions with a barrel wall which approximates a perfectly smooth surface the material constant σ_0 is an adequate (over) estimation of the uniaxial yield stress σ_y.

Paste extrusion in industry often uses non-axisymmetric systems. The Benbow-Bridgwater approach is easily adaptable. Modified versions of the model have proved adequate for many other more complicated axial extrusion arrangements, such as extrusion from a non-circular cross sectional barrel through a non-circular cross sectional die land [5]. Few researchers have investigated the extrusion from a barrel in non-axial directions. This study has chosen simple deviations from the axisymmetric arrangement shown in Figure 1 by adding dies aligned in the radial direction near the end of the barrel. The five different die arrangements A – E shown in Figure 2 have been studied.

Experimental stress and flow rate results have been obtained over a range of piston velocities. Characterization of the model paste has confirmed that the paste undergoes plug flow in the die land, and has provided material constants. A model to predict the extrusion pressure and paste flow for each of the five arrangements has been developed through extending the Benbow-Bridgwater model. This model successfully predicts the observed extrusion pressures, but gives little insight into the flow patterns.

MATERIAL STUDIED

A model agrochemical paste based on talc (magnesium silicate) was studied. The paste acts as a carrier for the small fraction of active ingredients which import crop protection *etc*. The paste formulation is given in Table 1. The talc particles (Table 2; Figures 3 and 4) are soft platelets whose lubricating properties render this paste suitable for extended investigation as they cause little attrition of the apparatus. Both Morwet components are surfactants which modify the rheology of the liquid phase, and are used at concentrations higher than the respective critical micelle concentrations.

The water contents of the constituents were obtained by drying triplicate samples and taking the mean. The water fraction by weight of the paste is calculated as 0.180, while the mean of triplicate samples from five separate batches of paste was calculated as 0.176. As might be expected, some drying of the paste occurs during production and handling. All of the Morwet was observed to go in to solution with the liquid phase thus the liquid phase fraction by weight of the paste can be calculated as 0.292. The density of a Morwet solution prepared with the fractions of Morwet and water shown in Table 1 was measured as 1160 kg/m^3. Using the density of talc given in Table 2 the liquid phase fraction by volume for the paste with no air entrainment is calculated as 0.507 and the density is 2020 kg/m^3.

The model talc paste was prepared in batches following a procedure outlined by Rough and Saracevic [6]. The dry talc and surfactant constituents were mixed together in a planetary mixer to evenly distribute the materials and gently break up any large agglomerates. The water was then gradually poured in with the dry constituents and mixed further to form a well distributed solution with the surfactant. This wetted the surface of the talc particles and bound them together. The resulting wet powder was twice pugged through the mixer's mincer attachment, breaking down small agglomerates and compacting the powder in to soft cylindrical pellets of length ~ 10 mm and diameter ~ 4 mm. The final paste was then left to relax in a hermetically sealed polythene bag before use. Paste was always used on the same day as it was produced.

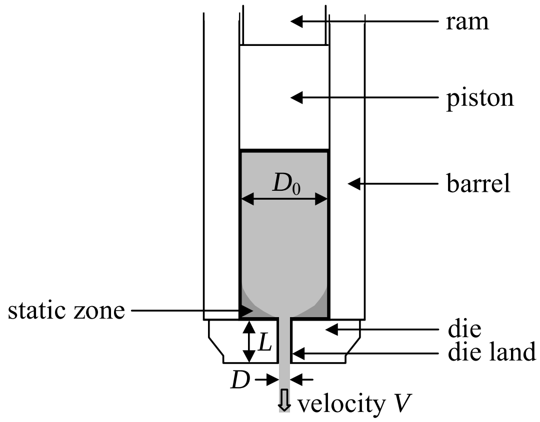

Figure 1 : Cross-section of an axisymmetric ram extruder with a square entry die

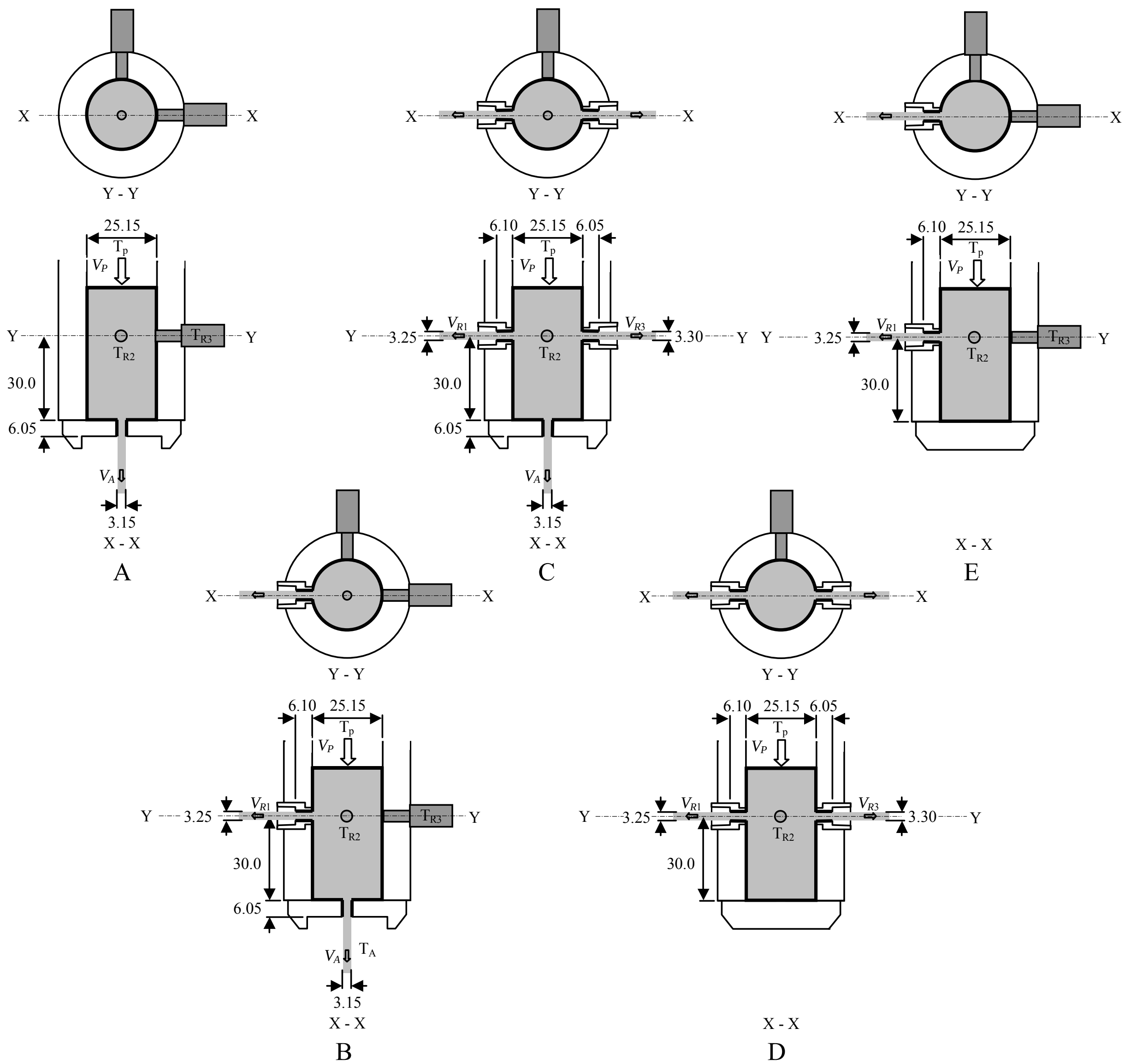

Figure 2 : Cross sectional views of extruder and pressure transducer arrangements
Measured dimensions are shown in mm (± 0.025 mm). T denotes pressure transducer or load cell.

Table 1 : Formulation of model talc paste

Constituent	Fraction (wt.)	Water content (wt. frac.)
Micro Talc AT	0.708	0.0039
Morwet EFW	0.0833	0.097
Morwet D425	0.0417	0.059
RO water	0.167	1.0

Table 2 : Manufacturer's data on Micro-Talc AT Extra

Mean particle size, μm	0.85
Specific surface, N_2-ads., $m^2\ g^{-1}$	7.70
Density, g cm^{-3}	2.90
Tamped apparent density, g cm^{-3}	0.34

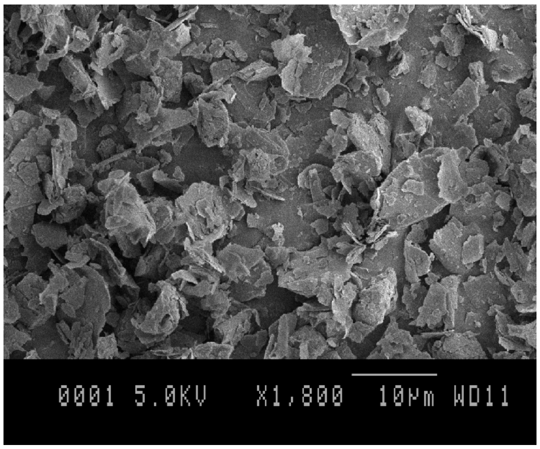

Figure 3 : SEM image of Micro-Talc AT Extra

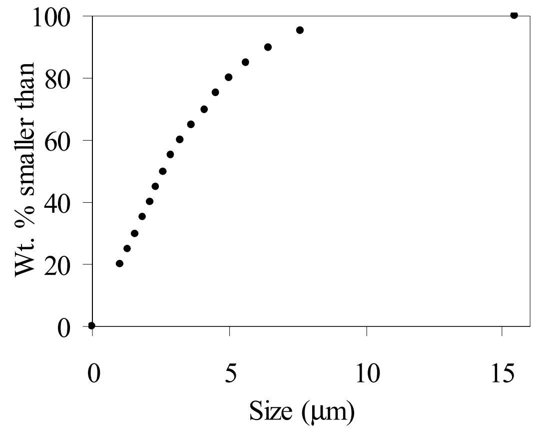

Figure 4 : Manufacturer's particle size distribution by wt. for Micro-Talc AT Extra

CHARACTERIZATION OF THE MODEL PASTE

The model talc paste was characterized to find material constants for use in modeling non-axisymmetric extruder arrangements. The characterization procedure of Benbow and Bridgwater [1] was followed; this uses the axisymmetric barrel and die arrangement of Figure 1 and yields the material constants as used in equation (4). The barrel had a length of 200 mm and a diameter D_0 of 25.10 mm (± 0.025 mm). Equation (4) suggests that if all other variables are held constant the extrusion pressure P is related to the die land length to diameter ratio L/D as a linear function with gradient $4(\tau_0+\beta V^n)$ and an ordinate intercept $2(\sigma_0+\alpha V^m)\ln(D_0/D)$. Studying the variation of gradient and ordinate intercept with extrudate velocity V provides data to which the material constants σ_0, α, m, τ_0, β and m can be fitted.

Ten different experimental runs were carried out in triplicate. Two sets of five dies were used with die land diameters of 2 mm and 3 mm. Each die within a set had a different die land length to diameter ratio (L/D); values of 2, 4, 8, 12 and 16 were used. A series of nine piston velocities were used over the duration of each run; 0.833, 0.667, 0.500, 0.333, 0.167, 0.0833, 0.0333, 0.0167, 0.833 mm/s. If the paste is incompressible, the extrudate velocity is a factor A_0/A greater than the piston velocity, where A_0 and A are the cross-sectional areas of the barrel and die land respectively. The maximum stress experienced by the paste is the same for each of these velocity periods since the fastest velocity was used first. This velocity was repeated at the end to assess how much extrusion conditions have changed over the course of the run.

The Benbow-Bridgwater equation (4) predicts the pressure required to extrude a paste by considering an energy balance of the work done by the piston and the work done in deforming the paste and overcoming friction in the die land. Thus in a characterization run it was the mean axial stress on the piston due to deformation and friction in the die land which was of interest. The piston will in addition have to do work against any wall friction in the barrel. For a perfectly smooth barrel the mean axial stress on the piston will be constant as the piston approaches the die until the point where the flow pattern near the die starts to change. Over all thirty runs the mean decrease of the mean axial stress on the piston from the first to last 0.833 mm/s velocity period was eight per cent. Other approaches to measuring the extrusion pressure are either prohibitively complex or time consuming, thus mean axial stress on the piston (with its associated error) was accepted as the extrusion pressure.

A screw action strain frame was used to drive the ram and piston through a displacement of 100 mm. An attached unit and a PC controlled the strain frame's cross bar movement, and thus the piston velocity, as well as capturing piston force and displacement data against time.

For each extrusion run a 140 g load of paste pellets was weighed out and manually compacted into the barrel with a blank die at its end. The piston was then used to precompact the material with a force of 5 kN (a mean axial stress of 10 MPa) applied for five to ten seconds which was thought to be sufficient to expel any entrained air. A plug of compacted paste approximately 140 mm in length was left in the barrel. The blank die was then replaced with the appropriate characterization die. The piston was lowered to make contact with the paste plug with a force of 0.5 kN and the characterization run commenced.

The extrusion pressure-time profile such as that shown in Figure 5 showed noticeable transients when the piston velocity was changed, presumably due to a combination of machine adjustment, elastic effects and changes in flow pattern. A steady state was reached relatively quickly and the mean value of extrusion pressure in these regions was used for characterization.

The extrusion pressures associated with each different extrudate velocity can be combined and plotted against the die land length to diameter ratio (Figure 6). A straight line fits reasonably well to these data, as is suggested by equation (4). The ordinate intercept (P_1) and gradient (P_2) were fitted by minimizing the sum of the squares of the normalized errors. Equations (2) and (3) allow values for the bulk stress $\sigma_0 + \alpha V^m$ and wall shear stress $\tau_0 + \beta V^n$ to be found from P_1 and P_2. It is apparent from Figures 7 and 8 that the data for both die land diameters coincide with each other, suggesting that the modeling approach used is appropriate. $\sigma_0 + \alpha V^m$ and $\tau_0 + \beta V^n$ both show a significant rate dependence. The material's resistance to change in cross-sectional area in the die entry can be approximated as having a yield value and then increasing linearly with extrudate velocity. The wall shear stress exerted on the material by the boundary layer can be approximated as being dependent on the extrudate (slip) velocity as a power function with no yield value. Appropriate values for the four material constants σ_0, α, β, n were found by minimizing the sum of the squares of the normalized errors, and are presented to two significant figures in Table 3.

Figure 9 shows a comparison of the means of the triplicate experimental extrusion pressures and the fitted Benbow-Bridgwater model for both die land diameters, with selected error bars covering the range of the three extrusion pressures. The root mean square normalized error over all the data points for both die land diameters is calculated as 0.16. The Benbow-Bridgwater characterization method provides a simple model of the material, but the accuracy of predicted experimental extrusion pressures in axisymmetric systems should not be expected to be any better than around 20 per cent.

If the material's resistance to cross-sectional change in the die entry $\sigma_0 + \alpha V^m$ is taken to be equal to the uniaxial yield stress of the material at the associated strain rate, then Tresca's yield criterion suggests that the maximum shear stress at this rate of strain $\tau_{y,bulk}$ is $(\sigma_0 + \alpha V^m)/2$. Thus the shear yield stress of the bulk material $\tau_{0,bulk}$ could be taken as $\sigma_0/2$. Plug flow in the die land the requires the wall shear stress τ_{wall} ($\tau_0 + \beta V^n$) to be less than the bulk shear yield stress of the material $\tau_{0,bulk}$. Figure 10 shows this to be true, thus the Benbow-Bridgwater characterization is consistent with plug flow in the die land. Figure 10 further shows that the ratio of die land wall shear stress τ_{wall} to the die entry maximum shear stress $\tau_{y,bulk}$ increases monotonically from zero to a value of 0.3 at an extrudate velocity of 0.02 m/s, after which the ratio changes little.

EXPERIMENTAL METHOD NON-AXISYMMETRIC EXTRUSION

The experimental method and equipment used for the non-axisymmetric extrusion was generally the same as that used for the material characterization. The notable differences were; a different barrel was used (of length 190 mm and diameter 25.15 ± 0.025 mm), paste was not precompacted prior to a run due to the difficulty of blanking the radial dies (resulting in the initial paste plug length in the barrel being approximately 180 mm), each velocity was performed as a single run, and pressure transducers were used to establish the extrusion pressure.

For each of the five die arrangements shown in Figure 2 at least six separate runs were carried out in triplicate at different piston velocities. It was found that the decrease in axial stress on the piston over the extrusion run for these runs was considerably larger than was observed in the characterization runs. Whereas in a characterization run the mean decrease in stress was eight per cent, a typical value for the multi-hole extrusion runs was twenty-two per cent. This value was deemed too great to allow the mean axial stress on the piston to be used as a measure of the extrusion pressure. For this work the extrusion pressure was taken to be the radial stress measured by pressure transducers located in the same plane as the radial dies (Figure 2). It is not clear how exactly the radial stresses measured relate to the extrusion pressure, but other results in the laboratory suggest that the difference is not great [7]. The extrudate from each die was collected over the duration of each run and weighed to give an indication of the flow rate through each die.

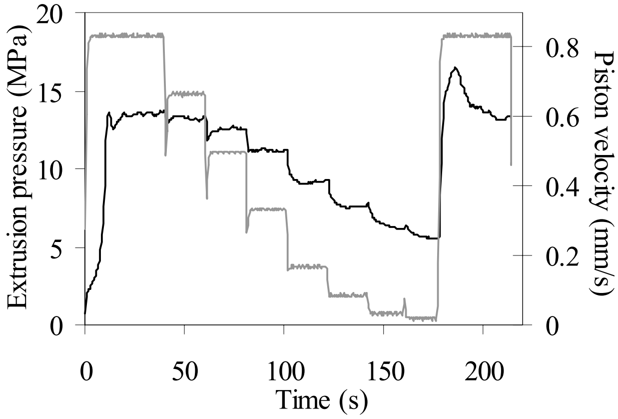

Figure 5 : Extrusion pressure and piston velocity against time   D = 3 mm, L/D = 16
— extrusion pressure
— piston velocity

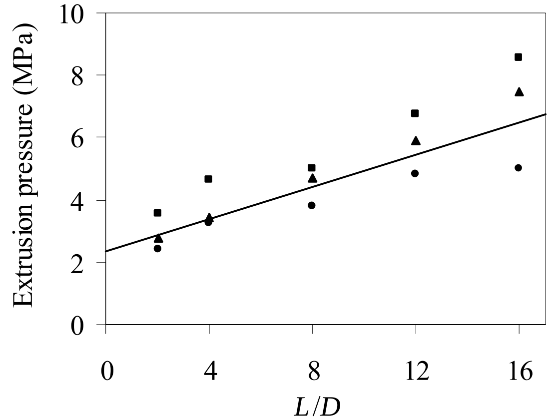

Figure 6 : Extrusion pressure against L/D
D = 3 mm, V = 0.00583 m/s
● ▲ ■ independent sets of data
— linear fit

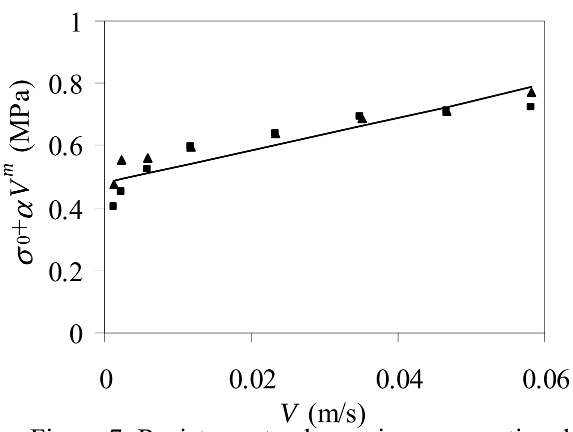

Figure 7: Resistance to change in cross-sectional area in the die entry against extrudate velocity
— parameter fit
▲ D = 3 mm   ■ D = 2 mm

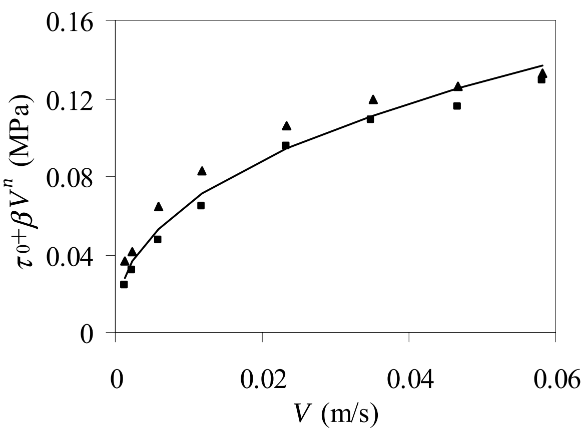

Figure 8 : Wall shear stress against extrudate velocity
— parameter fit
▲ D = 3 mm   ■ D = 2 mm

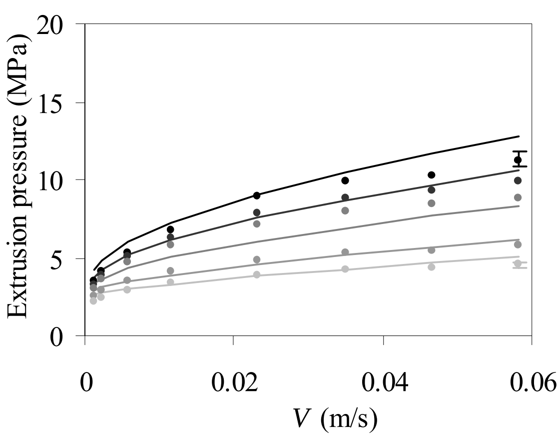

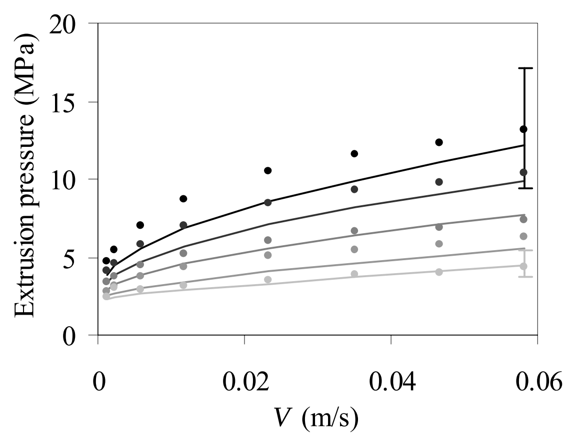

Figure 9 : (i) Extrusion pressure against extrudate velocity
— fitted model
● mean of triplicate experimental data
L/D = ● 16 ● 12 ● 8 ● 4 ● 2, D = 2 mm

(ii) Extrusion pressure against extrudate velocity
— fitted model
● mean of triplicate experimental data
L/D = ● 16 ● 12 ● 8 ● 4 ● 2, D = 3 mm

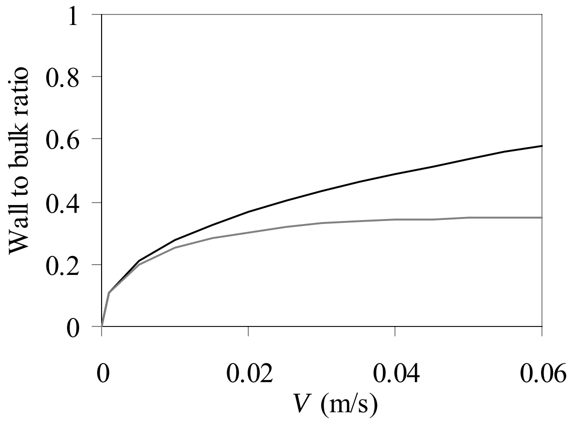

Figure 10 : Comparison of wall to bulk behaviour against velocity

—— $\tau_{wall}/\tau_{0,bulk}$

—— $\tau_{wall}/\tau_{y,bulk}$

Table 3 : Model talc paste constants

Material constant	Fitted value
σ_0, MPa	0.48
α, MPa (m/s)$^{-1}$	5.2
m	(1)
τ_0, MPa	(0)
β, MPa (m/s)$^{-n}$	0.44
n	0.41

MODELLING NON-AXISYMMETRIC PASTE FLOW

The Benbow-Bridgwater method outlined above can easily be adapted to predict the extrusion pressures and die flow rates in multi-die extrusion in a manner similar to that of Benbow *et al.* [5]. If all of the dies were identical, the method would predict that the flow rates through all dies be identical. The variation in the predicted flow rates is due to the measured differences between each of the dies. The analysis predicts the rate of work required to change the cross-sectional area of the flow from the barrel to the die land, and the rate of work required to overcome friction in the die land. Take arrangement C; suppose that at a plane where no deformation has yet occurred and the paste is flowing as a plug in the barrel, flow through a fraction θ_A of the cross-sectional area continues to flow through the axial die. Similarly flow through a fraction θ_{R1} continues to flow through radial die 1, and the remaining fraction θ_{R3} continues to flow through radial die 3. Bulk and wall paste properties associated with each of these three flows can be calculated using the Benbow-Bridgwater characterization parameters (Table 3) and the extrudate velocity of each flow. The work rate W_A associated with the flow through the axial die is

$$W_A = \theta_A \pi (D_0/2)^2 V_p \left(\sigma_0 + \alpha V_A{}^m\right) \ln\left(\theta_A D_0{}^2 / D_A{}^2\right) + \pi D_A L_A V_A \left(\tau_0 + \beta V_A{}^n\right) \tag{7}$$

where the extrudate velocity through the axial die is given by

$$V_A = \left(\theta_A D_0{}^2 / D_A{}^2\right) V_p \tag{8}$$

and similar equations follow for the work rates associated with the flows through the two radial dies. Equating the sum of these three work rates with the rate of work done by the piston $\pi(D_0/2)^2 V_p P$ allows the extrusion pressure P to be calculated for a given flow distribution between the three dies. A spreadsheet solver function was used to find the optimal flow distribution by minimizing P through varying θ_A, θ_{R1} and θ_{R3}. This same method may be applied to the other multi-die extrusion arrangements B and D.

RESULTS

Stress data from a typical extrusion run are presented in Figure 11 where the axial die and one radial die are in use (arrangement B) and the piston is travelling at a velocity of 1 mm/s. The extrusion run can be divided into two distinct regions. The first is a transient region where compaction of the paste occurs, the flow pattern of the paste is established and any elastic responses occur. The second is a steady state region. During the steady state region the mean axial stress on the piston is clearly seen to decrease during the course of the run, as was mentioned previously. This is presumed to be due to the effect of friction on the paste against the barrel wall boundary layer. The radial stresses measured by transducers T_{R2} and T_{R3} fluctuate only slightly within the steady state region and largely in phase with each other. The mean of the measured radial stresses was calculated and taken as the extrusion pressure. In cases such as this where two radial stresses were measured (arrangements A, B, E) the two means were typically within a few per cent of each other.

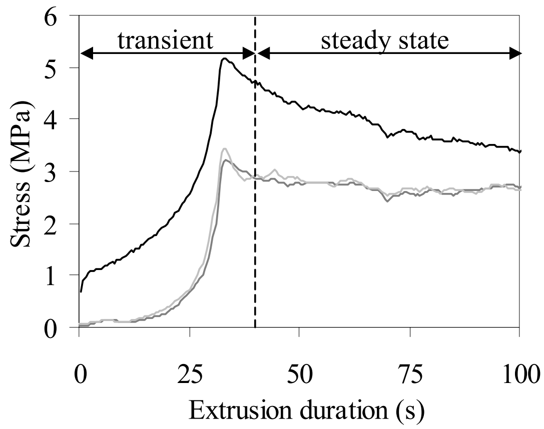

Figure 11: Stress against extrusion duration
Die arrangement B. V_p = 1 mm/s
mean axial stress on piston
radial stress on barrel at T_{R2}
radial stress on barrel at T_{R3}

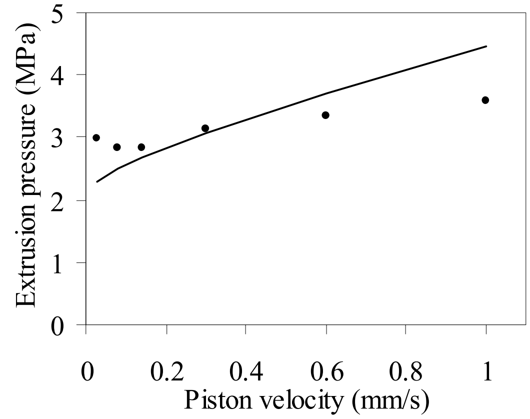

Figure 12 : Extrusion pressure against piston velocity

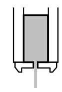

Die arrangement A
model prediction

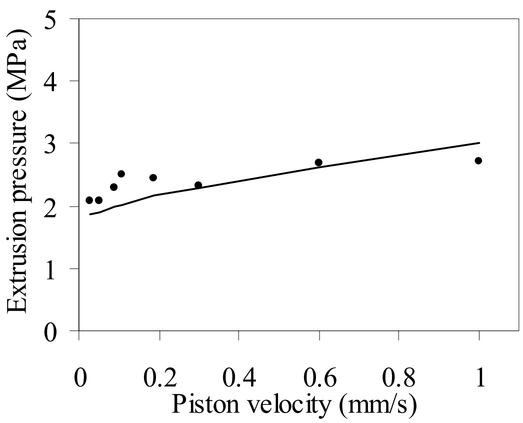

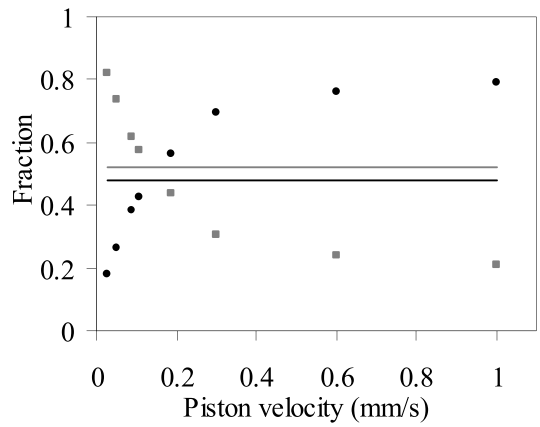

Figure 13: (i) Extrusion pressure against piston velocity

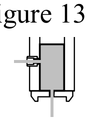

Die arrangement B
model prediction

(ii) Flow distribution against piston velocity
Die arrangement B
● axial die ■ radial die 1

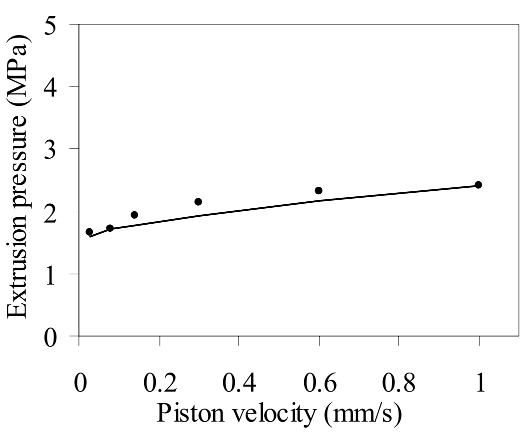

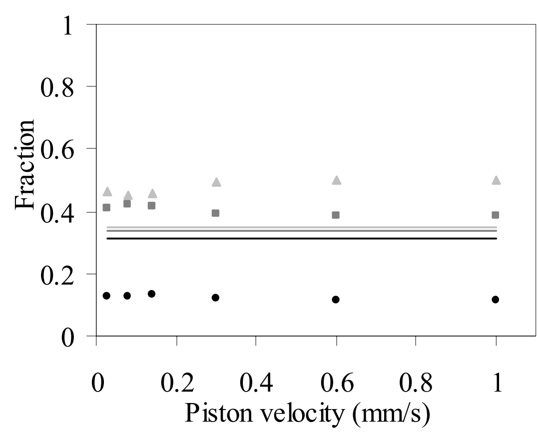

Figure 14: (i) Extrusion pressure against piston velocity

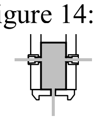

Die arrangement C
model prediction

(ii) Flow distribution against piston velocity
Die arrangement C
● axial die ■ radial die 1 ▲ radial die 3

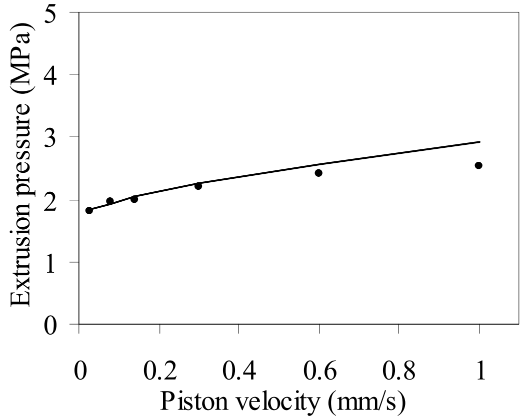

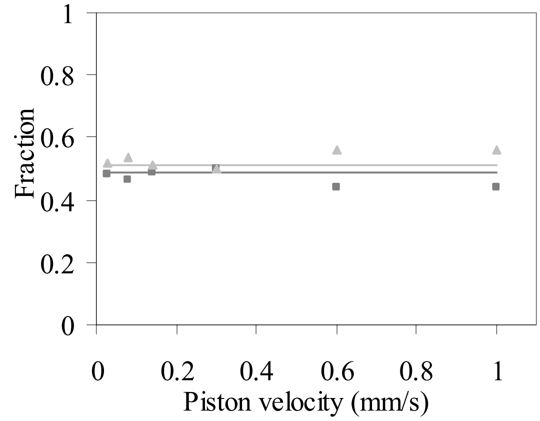

Figure 15: (i) Extrusion pressure against piston velocity
Die arrangement D

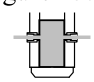

—— model prediction

(ii) Flow distribution against piston velocity
Die arrangement D
■ radial die 1 ▲ radial die 3

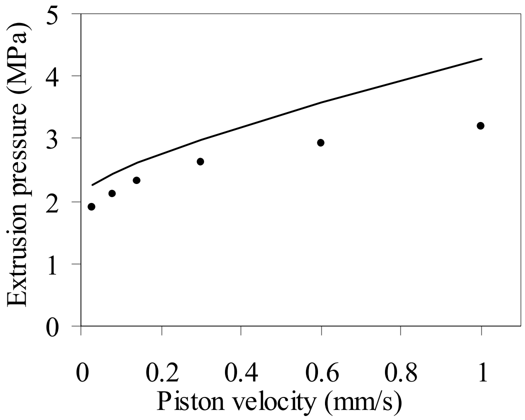

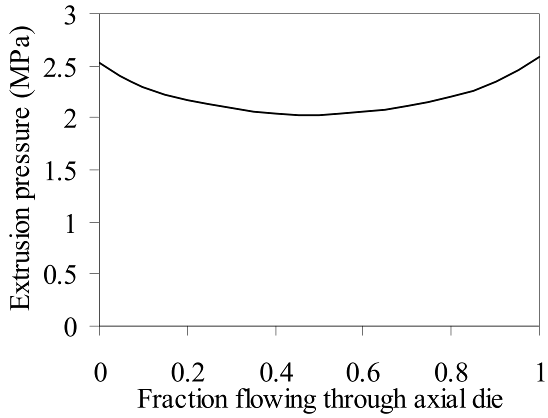

Figure 16: Extrusion pressure against piston velocity
Die arrangement E

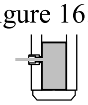

—— model prediction

Figure 17 : Predicted extrusion pressure against fraction of flow through axial die
Die arrangement B, $V_p = 0.11$ mm/s

The means of the triplicate experimental extrusion pressures and the paste flow distributions are shown, along with the Benbow-Bridgwater model predictions, in Figures 12 – 16 for the five die arrangements A – E respectively. It is evident that the model appears to satisfactorily predict both the magnitude and trend of the extrusion pressure. That the agreement is close in some cases is probably fortuitous given the previously discussed inaccuracies of the material constants. This result suggests that the redundant work expended when extruding through a radial die is similar in magnitude to the redundant work expended when extruding through an axial die. The model only approximately predicts the flow distribution for the two-radial-die arrangement D, for arrangement C the model does not predict the magnitudes of the experimental flows, and for arrangement B the model neither predicts the magnitudes nor the trends of the experimental data which display dramatic changes as the piston velocity is varied.

The Benbow-Bridgwater model gives little insight in to why the observed flow patterns developed. The predicted variation of extrusion pressure against fraction of flow thorough the axial die for the axial and radial 1 die arrangement B with a piston velocity of 0.11 mm/s is shown in Figure 17. The predicted extrusion pressure is significantly affected by the flow pattern. If the predicted extrusion pressure were only a weak function of flow pattern then it might be thought that minor factors neglected in the model might strongly influence the actual pattern, but this hypothesis does not seem to be supported by the result.

Two insights are available in the given characterization and non-axisymmetric experimental data. It was evident in Figure 10 that the ratio of the wall shear stress to bulk shear stress $\tau_{wall}/\tau_{y,bulk}$ is sensitive to the extrudate velocity when below approximately 0.02 mm/s; above this extrudate velocity the ratio changes little. This corresponds with the observed variation of flow pattern with piston velocity. As the piston velocity is first increased large changes in the flow patterns may occur, but as the piston velocity is increased further and the ratio $\tau_{wall}/\tau_{y,bulk}$ approaches a constant the flow pattern becomes steady also.

It can be seen in Figure 12 where the extrusion pressure against piston velocity is presented for the arrangement of an axial die only A, that the extrusion pressure is approximately constant for the lowest three velocities, and greater than the extrusion pressures at the same velocities for arrangement E with only radial die 1. This suggests that under these conditions it is more efficient for the paste to flow out of the radial die than the axial die, whereas this is not true for higher piston velocities. These single die results are consistent with what is observed when the same two dies are used in arrangement B (Figure 13). Here the flow is seen to be predominantly through the radial die at low velocities and the extrusion pressure is approximately equal to the extrusion pressure for the radial die only (E). At higher velocities the efficiency advantage of the radial die diminishes and the flow pattern changes. The Benbow-Bridgwater modeling method does not contain the potential to model these subtleties.

CONCLUDING REMARKS

A model talc based paste has been proven useful for extrusion flow research and successfully characterized using the standard Benbow-Bridgwater method. It has been confirmed that the paste undergoes plug flow in a capillary. Flow in non-axisymmetric ram extruder die arrangements has been studied for this paste. It has been found that a simple adaptation of the Benbow-Bridgwater method can predict the magnitudes and trends of the experimentally observed extrusion pressures, but that the method is not sensitive enough to adequately predict the observed flow patterns.

NOMENCALTURE

Roman

A	cross-sectional area of die land
A_0	cross-sectional area of barrel
D	die land diameter
D_0	barrel diameter
L	die land length
m	die entry velocity index
n	die land velocity index
P	extrusion pressure
P_1	die entry pressure drop
P_2	die land pressure drop
T	pressure transducer
V	extrudate velocity
V_p	piston velocity
W	rate of work

Greek

α	die entry velocity factor
β	die land velocity factor
θ	fraction of flow
σ_0	die entry yield stress
σ_y	uniaxial yield stress
τ_0	die land wall yield shear stress
$\tau_{0,bulk}$	bulk yield shear stress
τ_{wall}	die land wall shear stress
$\tau_{y,bulk}$	bulk maximum shear stress
ξ	logarithm of the diameter ratio [$\ln(D_0/D)$]

Subscripts

A	associated with axial die
R1	associated with barrel wall position 1
R2	associated with barrel wall position 2
R3	associated with barrel wall position 3
p	associated with the piston

REFERENCES

1 Benbow, J.J. & Bridgwater, J. (1993), *Paste Flow and Extrusion*. Clarendon Press, Oxford, 25-44.
2 Ovenston, A. & Benbow, J. J. (1968), ‘Effects of die geometry on the extrusion of clay-like material’, *Transactions of the British Ceramic Society*, **67**, 543-567.
3 Benbow, J. J. (1971), ‘The dependence of output rate on die shape during catalyst extrusion’, *Chemical Engineering Science*, **26**, 1467-1473.
4 Horrobin, D. J. & Nedderman, R. M. (1998), ‘Die entry pressure drops in paste extrusion’, *Chemical Engineering Science*, **53** (18), 3215-3225.
5 Benbow, J. J., Jazayeri, S. H. and Bridgwater, J. (1991), ‘The flow of pastes through dies of complicated geometry’, *Powder Technology*, **65**, 393-401.
6 Rough, S. L., Saracevic, Z. (1997) ‘Final report on paste extrusion work for Zeneca Agrochemicals’, Department of Chemical Engineering, University of Cambridge.
7 Amarasinghe, A. D. U. S. (1998), Interpretation of Paste Extrusion Data. PhD Thesis, University of Cambridge, 36-39.